Journal of Structural Geology, Vol. 6, No. 3, pp. 321 to 329, 1984
Printed in Great Britain

0191-8141/84 $03.00 + 0.00

Simulation of deformation of lattices: point-to-point analysis and applications*

M. MISSERI and J. L. VIGNERESSE

Laboratoire de Tectonophysique, Université de Nantes,
44072 Nantes Cedex, France

(*Received* 30 *June* 1982; *accepted in revised form* 3 *October* 1983)

Abstract—When applied to homogeneous rocks, the statistical technique of autocorrelation helps in visualizing the preferential alignment of mineral barycenters. We examine the behaviour of each element within a regular lattice deformed in either simple or pure shear. Preferential directions immediately appear depending upon the relative orientation of the shear or flattening plane with respect to the lattice. Autocorrelation amplifies these directions (either one direction with a high intensity signal or two directions with weak intensity signals). They depend on the geometrical shape of the elementary mesh of the lattice which is changing during the deformation. From the autocorrelated diagram, geometrical parameters of the elementary mesh can be estimated. Resulting from the numerical simulations, graphs are constructed which provide strain estimates in the case of simple shear. Application to natural rocks deformation is given in the case of simple-sheared peridotites.

INTRODUCTION

VARIOUS methods are available for estimating strain in deformed rocks. Most of them require the existence of continuously deforming finite markers distributed over the whole field to be analysed. In sedimentary or low-grade metamorphic rocks this condition may be satisfied by pebbles, reduction spots or deformed fossils. In igneous rocks, strain patterns can be estimated only in a few cases, using sophisticated physical methods such as magnetic susceptibility anisotropy or X-ray texture analysis. For instance, in peridotites, only qualitative strain estimates have been made so far (Nicolas & Poirier 1976).

Our starting assumption is that, in deformed rocks, a strain sensitive pattern exists in the crystal distribution, which is difficult to discern. In the most favourable cases, clustering of barycentres from each crystal within a lattice or within an aggregate immediately appear as a result of the deformation (Fig. 1). Therefore signal-processing techniques (Robinson 1962, Agterberg 1974, Kulhanek 1976) are used to extract the signal (the bulk

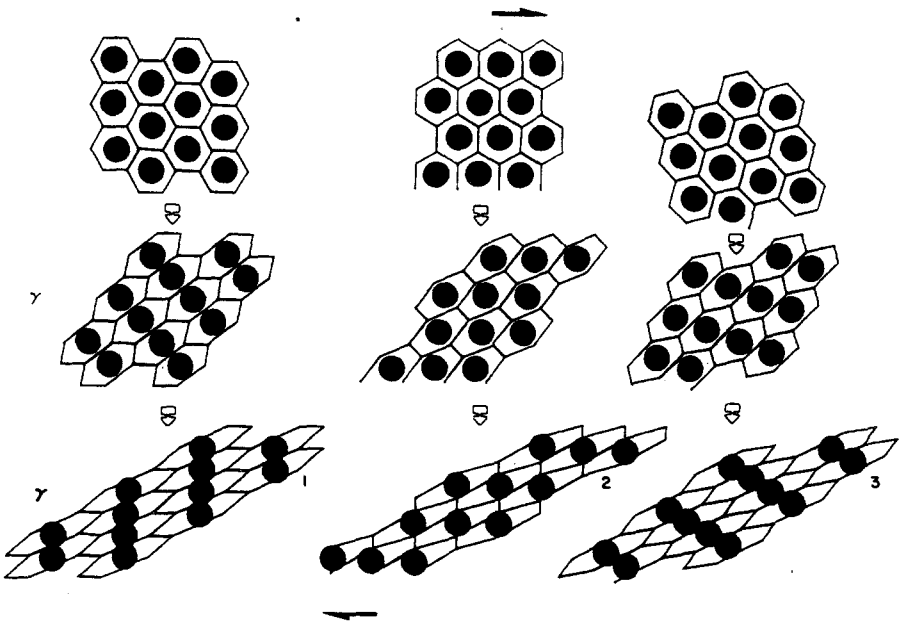

Fig. 1. Hexagonal lattice deformation. Linear clusters depend upon the angle between the stacking plane and the shearing plane. They rotate according to Ramsay's equations (1967) with increasing strain. Autocorrelation would amplify those clusters. In the case of 1 and 3 one direction rotates according to the shear deformation; in case 2 two directions are present with less defined characters.

* Presented at the International Workshop *Strain Patterns in Rocks* at Rennes, 13–14 May 1982.

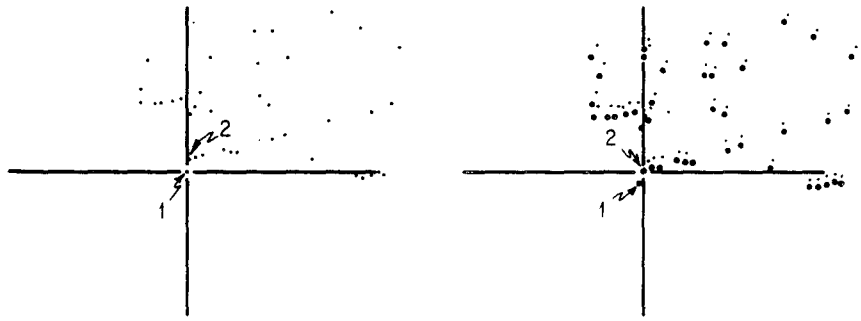

Fig. 2. Method for obtaining an autocorrelation diagram in binary-points representation. The method consists of translating the origin at each successive point and plotting the remaining points.

strain) from the surrounding noise. A signal is defined as any elected trace of what is considered to be representative of the process under analysis. In deformed peridotites, we have considered (Misseri & Vigneresse 1982) spinel grain distribution as the output signal of a strain acting on the whole rock. In the present paper, we generalize this concept considering that the pattern given by the distribution of each grain barycentre in the rock still records the strain history of the rocks.

Signal-processing techniques commonly use statistics and/or transformation from the usual time or spatial domains to the frequency domain (Robinson 1962). The present problem is to amplify a signal in order to perceive it, since the signal-to-noise ratio is low and filtering techniques are not helpful; one possibility is to increase the order of statistics which describes the phenomenon since perception studies have demonstrated that human vision is most aware of second-order statistics (Julesz 1962). For instance when data present similar first-order parameters (arithmetic means as an example) then, by examining their second-order parameters (variances), small variations within the sample blow up. Those second-order statistical techniques incorporate quadratic functions of the signal components. Correlation is such a process.

METHOD

Amongst the correlation techniques, autocorrelation and crosscorrelation are the most usual. Crosscorrelation measures the degree of similarity between two functions, whereas autocorrelation is the measure of the similarity of a signal with itself when shifted along the sampling interval. If each value of the function at a sampling point is taken as a component of the signal, vector notation may be applied to the signal. Mathematical formulation of the autocorrelation is then (Agterberg 1974):

$$a_i = \sum_{j=1}^{n} s_j \cdot s_{j+i} \quad \text{or} \quad \boldsymbol{a} = \boldsymbol{s} * \boldsymbol{s},$$

where a_i is the ith component of the autocorrelated signal, with shift i, and s_j is the jth component of the signal.

The autocorrelation process is highly simplified when dealing with a distribution of points. Here the function under analysis is represented by binary data: (0 for absence and 1 for presence of the point). In such a case, computing the autocorrelated diagram results in taking one point as the origin of a new coordinates system and plotting the remaining points into this system (see Fig. 2 in the case of a natural rock sample). Such methods have been previously described (Barbier & Leymarie 1972, Brun 1980). Applications to deformation are described in Fry (1979), Hanna & Fry (1979) and Ribeiro *et al.* (1983).

In the above mentioned papers, a point distribution is mainly used for estimating the strain components acting on a finite marker of non-nul area (i.e. the area of which is non-negligible with respect to the size of the sample). The idea is to use the relative distribution of markers to determine the average strain. The distribution may be pseudo-random or resulting from a double Poisson process (Ribeiro *et al.* 1983), since the markers are of finite area and thus imply no mutual overlapping. So the results of autocorrelation may differ, depending on the kind of point distribution.

SIMULATION OF THE DEFORMATION OF A LATTICE

A homogeneous finite deformation acting upon a given lattice can be simulated by numerical and geometrical means. Numerical simulation of the deformation is done through computing techniques described in Appendix. Incremental deformation is performed with a fixed shearing direction. The influence of the angle between the packing frame and the shear direction is also examined by rotating the initial lattice orientation. A triangular lattice has been chosen for the computation since it can be viewed as the most general case and can be referred to from any other lattice system. Clustering of barycentres in a regular lattice may occur in some favorable case only through geometrical simulation of the deformation (Fig. 1). In order to reinforce the image, the deformed states of a regular lattice are autocorrelated and the resulting computed function is plotted (Fig. 3).

A periodical character of the autocorrelated signal is found when the initial signal is periodic. Autocorrelation

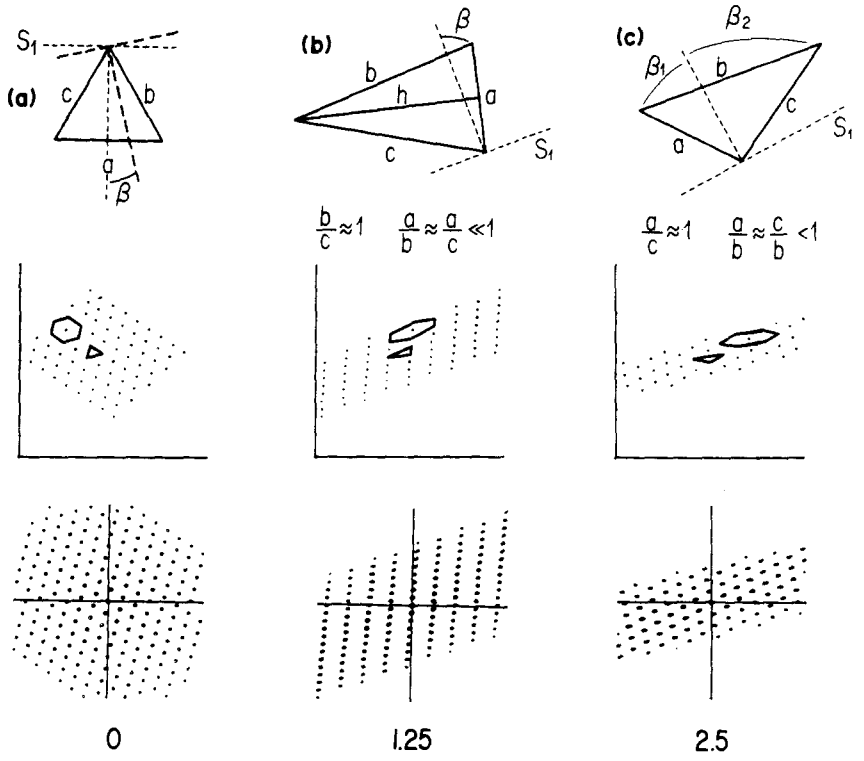

Fig. 3. Evolution of a triangular (hexagonal compact) lattice during simple shear; the cell and the elementary triangular mesh are outlined. Autocorrelation diagrams of the deformed lattice are presented. Note the change from (a) nodal character ($\gamma = 0.$) to (b) one well defined linear cluster ($\gamma = 1.25$) and (c) two less defined linear clusters ($\gamma = 2.5$). The basic triangular cell is presented at different stages with the corresponding geometrical parameters. Due to plotter edge effects, an apparent loss of points occurs in the autocorrelation diagram on highly deformed cases.

is a central symmetric process which, when applied to a signal, results in the combination and amplification of the various anterior symmetry properties of the signal. For instance, a regular lattice of nodes constructed from the intersection points of periodical lines gives an autocorrelation diagram of nodes with the same periodicity. In the case of a triangular lattice, cell edges are oriented with a triadic symmetry pattern, (plane of symmetry rotated 120°); then the resulting autocorrelation diagram presents first-order directions (least distances between points in the cell) having the anterior symmetry pattern. It is therefore nodal in character with triadic pattern. In the case of linear periodic structures with different azimuthal frequencies, the major direction to appear in the autocorrelated signal is the one for which the azimuthal frequency is the highest; that is, the direction along which the points are the closest to each other. In order to test numerous cases ranging from a regular lattice to a pseudo-lattice as in natural rocks, we use a triangular lattice in which we progressively allow points to depart from their theoretical mesh positions (Fig. 4a).

The spatial distribution of the initial points is the underlying condition which determines the shape of the autocorrelation diagram. If we start from a perfect lattice of points, the resulting autocorrelation diagram is nodal in character since the initial signal is nodal (Fig. 4a). When a slight departure from the node position is allowed for the points within the initial lattice frame, then the autocorrelated diagram progressively loses its nodal character and turns to linear clusters (Fig. 4b). If further departure is allowed for the points, they may attain a random distribution thus producing an autocorrelation diagram with no definite cluster. This can be understood when reminded that the autocorrelation process is a convolution process and therefore implies intimate multiplication/convolution reciprocity between frequency and spatial domains. In the frequency domain, a periodic mesh is represented by Dirac impulsions with frequency depending upon the mesh parameters. If a slight departure is allowed for the points, the frequency representation of the impulsions widens towards a Gaussian distribution. When a random distribution of points is obtained, the frequency distribution turns to a Poisson-like process which is flat in amplitude and incorporates infinite frequencies. Since convolution (autocorrelation also) is very sensitive to the data frequency distribution relative to sampling frequency (departure of the points with respect to their internodal distances), this explains why linear clusters were obtained in our case.

RESULTS

When a regular triangular lattice is processed we observe, after signal autocorrelation, the existence of linear clusters with preferred orientations. These linear clusters are induced by the lattice nature of the signal (Fig. 3a). This is a major difference from the preceding

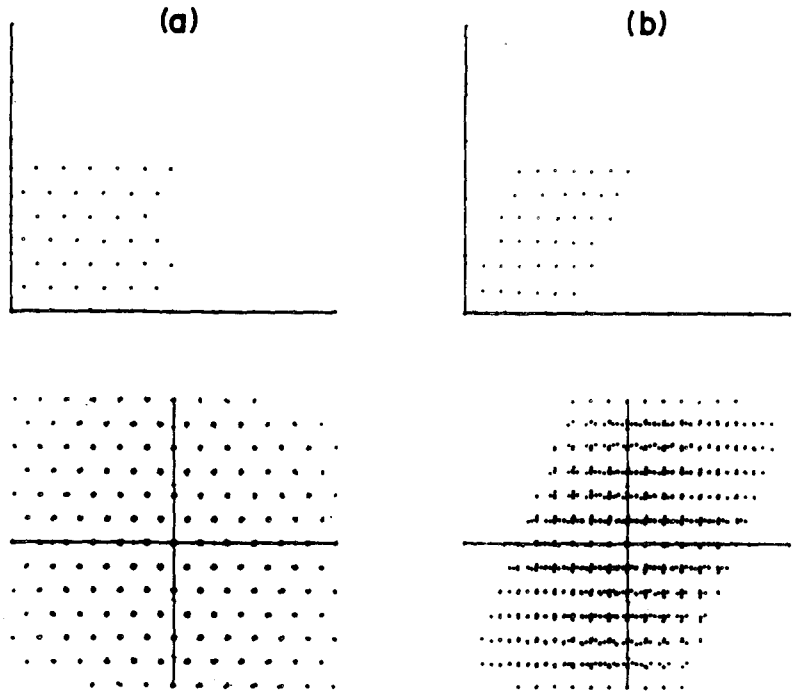

Fig. 4. Autocorrelation of a non-deformed (a) and a deformed (b) triangular lattice, in which the points slightly depart from their initial mesh position. Due to this departure, a change is observed from nodal to linear clustering of the autocorrelated points.

point-to-point methods (Fry 1979, Hanna & Fry 1979, Ribeiro *et al.* 1983), in which the random initial distribution of points results in a non-directional cluster within the autocorrelation diagram. During deformation of a regular lattice, the linear clusters rotate in orientation. For instance, in the simple-shear case, a cluster with orientation α with respect to the shear plane rotates to an angle α' in the deformed state. Relationship between the undeformed and the deformed directions of a given marker follows Ramsay's (1967) equation in the simple shear case

$$\cot \alpha = \cot \alpha' + \gamma \text{ with } \gamma \text{ the usual shear strain.}$$

In the case of moderate shear, the more drastic changes occur for directions located within 45° to the perpendicular to the shear plane.

Orientation and number of linear clusters

We found that the orientation of the linear cluster is basically dependent upon the spacing between two nodes in the lattice. In the elementary triangular mesh, the preferred direction of the linear cluster is the one derived from the direction along which points are the closest within the elementary starting triangle. We observe two major cases.

(a) *A single well-defined direction of cluster.* This corresponds (Fig. 3b) to the case in which the elementary triangle, after deformation, is reduced to an isosceles triangle in which one side (a) is much shorter than the other sides (b and c). In that case the sharpest cluster is encountered for $b/c = 1$ and $a/b = a/c \ll 1$.

For strain determination, the three necessary parameters are β (angle between the perpendicular to the foliation and the side a which is parallel to the cluster direction) and the values a and h (the height of the deformed triangle which is also the value of the shortest side in the triangle periodicity of the linear cluster).

(b) *Two poorly-defined linear clusters.* In such a case (Fig. 3c), the signal corresponds to an irregular triangle in which two sides are nearly equal but both are much shorter than the remaining side ($2a/c = 1$ and $a/b = c/b \ll 1$). Two linear clusters are encountered, each one oriented with respect to the shear plane with angles β_1 and β_2 equal to the angle of both adjacent sides of the triangle with the perpendicular to the foliation plane. Then four parameters are needed for the interpretation. They are: the angles β_1 and β_2, and the short sides a and c of the triangle.

When computing the parameters of a deformed elementary triangular mesh within a triangular lattice as a function of the strain, variations of the above quoted parameters in either distance and orientation are observed (cf. Appendix). Since the shortest side in the deformed triangle may vary in orientation with respect to the strain components, the linear clusters resulting from autocorrelation follow a law identical to that of the variations of the length of the sides during deformation. When starting from a regular triangular lattice, one well-defined cluster in the autocorrelated diagram appears. Its orientation is that of the shortest side within the triangular mesh which roughly corresponds to the orientation of the side of the triangle lying within a small sector relative to the shortening azimuth. The rotation of the short side in the triangle may precede the rotation of the shortening azimuth; as soon as the short side enters into the elongation sector, it quickly increases in size. At this point, it may be large enough to become the

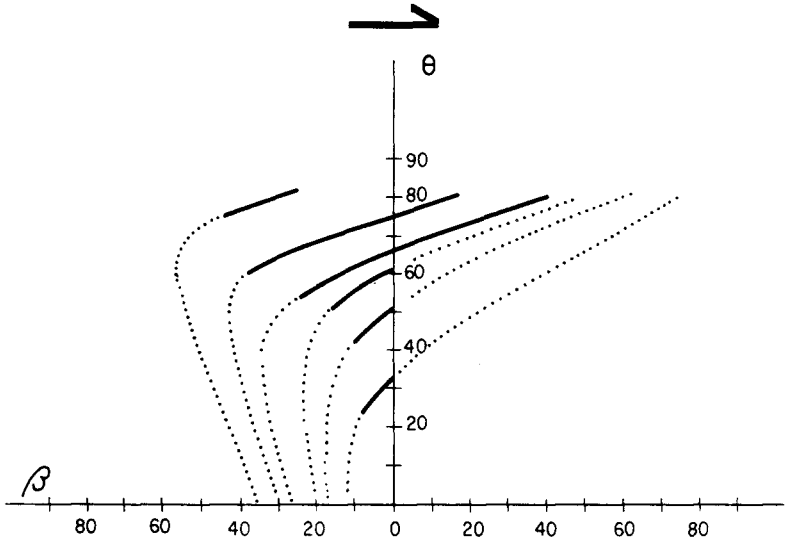

Fig. 5. Templates displaying which orientation the well defined linear cluster presents depending upon the cell orientation β and the strain rate of simple shear. The initial lattice possesses an equilateral triangular cell in this case.

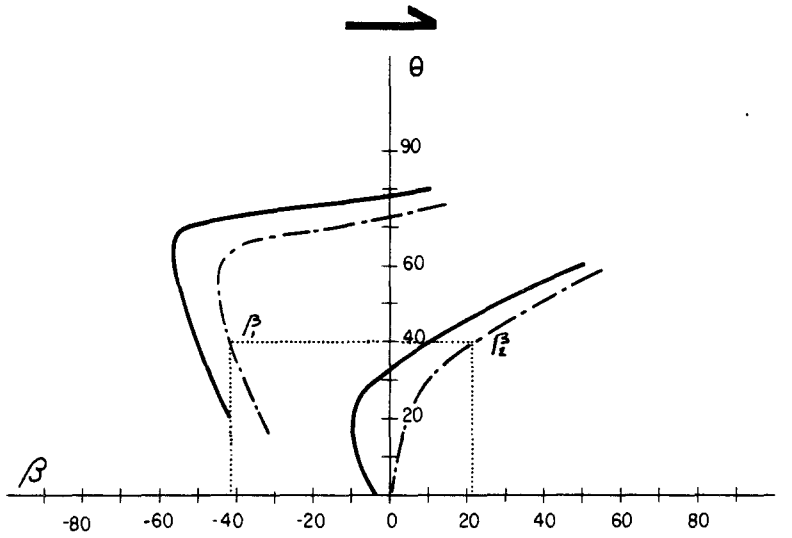

Fig. 6. Partial template for two less-defined linear clusters. Strain may be estimated if one knows the respective angles of the two clusters (β_1, β_2) with respect to the foliation plane. In this case, the initial lattice is an equilateral triangular.

second side in length within the triangle. As a result, drastic change occurs in the autocorrelation diagram evolving from a single linear cluster to two less defined clusters (Figs. 3b & c).

Starting from an initially equilateral cell, two types of theoretical templates are obtained depicting the possible range of clusters in the autocorrelation diagram as a function of the amount of strain. They depend on the kind of linear clusters observed during the autocorrelation process. In the first case (Fig. 5) only one well-defined direction is observed. In this case, however, determining the angle between the perpendicular to the foliation ($S1$) and the linear cluster is not sufficient to fully determine the strain and the shear nature, since the resulting angle β strongly depends upon the starting orientation of the marker. In the case of two weakly defined linear clusters, the values of both angles β_1 and β_2 of the linear clusters with the perpendicular to S1 plane theoretically fully determine the system, since two trajectories of curves in the template (Fig. 6) are used. We do not present in Fig. 6 a full template for the case of two weak intensity clusters because there are too numerous cases to be taken into account. Furthermore, the angle of the packing frame with the shear direction complicates the interpretation. For these reasons, this case will not be described.

SIMULATION OF THE DEFORMATION OF A NON-REGULAR LATTICE

Geometrical deformation of various basic elementary triangles has been numerically simulated (cf. Appendix) to obtain deformation estimates from the autocorrelation diagram. The starting material consists of triangular elementary meshes of different shapes on which geometrical deformation is applied. Simple shear has been

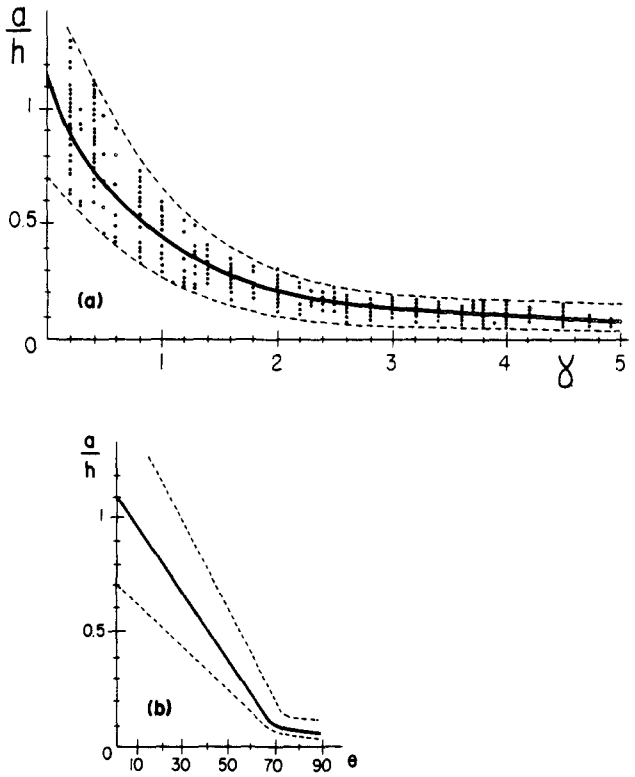

Fig. 7. (a) Curve displaying the computed values of a/h vs γ when simulating the pure shear deformation of a pseudo-equilateral triangle. The solid line is the mean curve for the whole data set, the envelope given by the dotted lines. (b) Values and envelope as in (a) but as a graph of a/h vs $\theta = \tan^{-1}\gamma$.

considered. The length and orientation of each side of the triangle which determine the autocorrelation clusters are computed as a function of progressive strain value. Results are identical to the case of a regular lattice, displaying linear clusters; however, the cluster character is more diffuse.

In order to avoid the ambiguity encountered in the case of a single linear cluster, a synthetic graph displaying the variations of combined parameters as a function of strain has been plotted (Fig. 7) from the geometrical parameters of a deformed triangle. The starting cell is equilateral to simulate a triangular lattice. Next, each summit is allowed to depart by up to 20% from its equilateral coordinates in a periodic lattice. This simulates a triangular pseudo lattice. This range of departure allows us to take into account most natural textures, provided no pronounced anisotropy or heterogeneity exists. The influence of the orientation of the packing plane with respect to the shear direction is also examined through incremental rotations of 10°. The total finite deformation is applied to the triangles by increments of $\gamma = 0.25$ in the case of a simple shear. During the simulation we consider the length of the sides of the triangle, their orientation relative to the shear plane, and the ratio of one side to each other; the height (h) of the triangle perpendicular to the shortest side is also computed. Tests are made to keep only the relevant deformed triangles which produce one well defined linear cluster (one side much shorter than the two adjacent other ones when the triangle is nearly isosceles) or two weak clusters (two adjacent sides nearly equal, the third side being much larger). The resulting list is impressive in volume (more than 5000 results). A second test consists in eliminating an abundant redundancy in the results, mainly due to a systematic rotation of the initial triangle through 10 increments over a 180° range. The resulting list, is then more tractable. The computed values of a/h for which an autocorrelation diagram with one well defined cluster is obtained are plotted as a function of γ. Results are shown in Fig. 7. As a function of the increasing amount of strain, the ratio a/h progressively decreases. Results are far more impressive when plotting the ratio a/h as a function of the angle $\theta = \tan^{-1}\gamma$ (Fig. 7). A linearly dependent curve may be fitted to the data and the obtained relationship is described by the equation

$$a/h = 1.12 - 0.015\,\theta$$

which is valid for values of θ smaller than 70°. The theoretical justification of such a linear relationship is not presented. Then, depending on the kind of produced autocorrelation diagram, namely if one well defined cluster or two less defined clusters are obtained, the knowledge of either the angle β and the value of a/h or the two angles β_1 and β_2 and the side lengths a and c, one may estimate the value of the strain by using the graphs of Fig. 5 and Fig. 7 or 6.

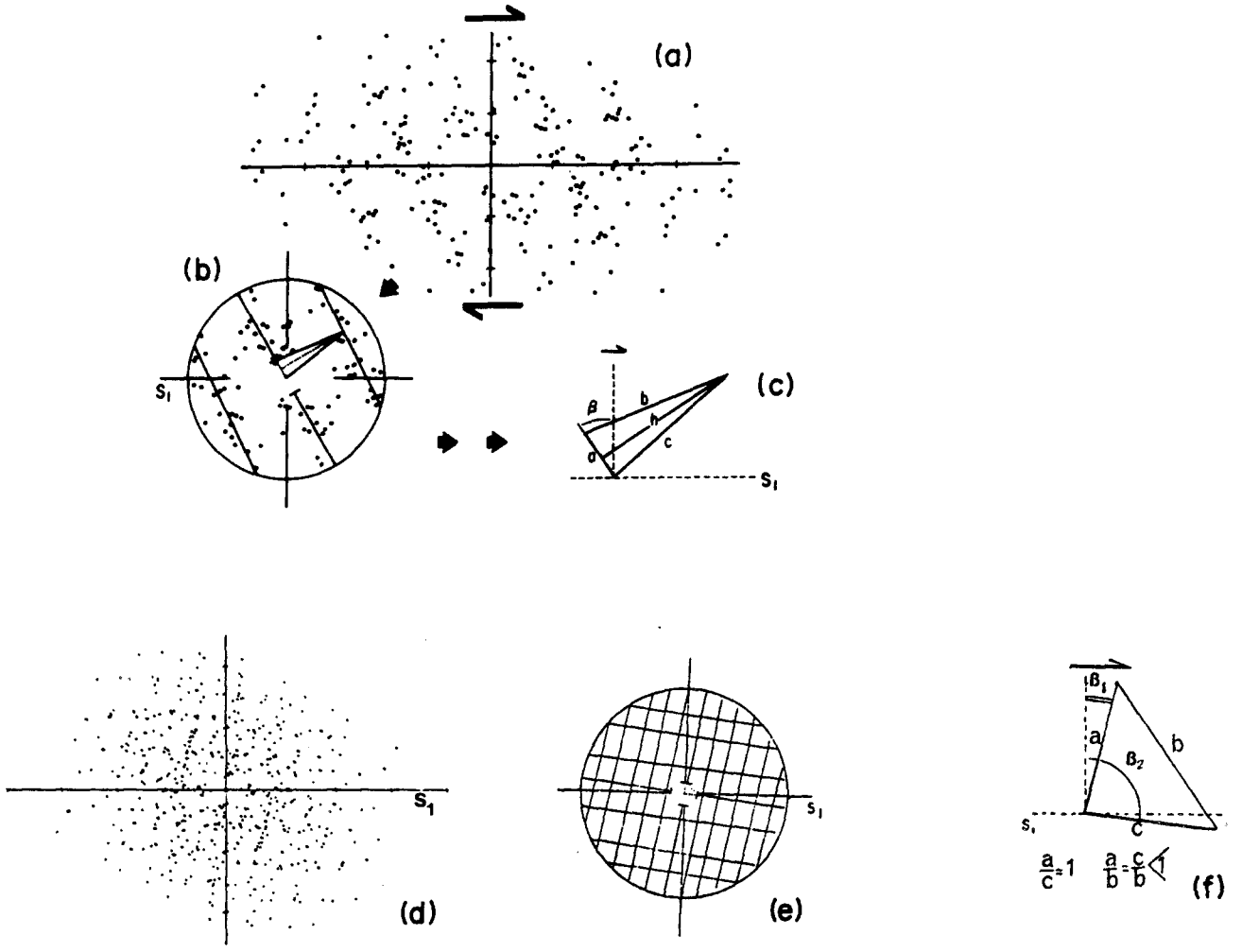

Fig. 8. Autocorrelation diagram of a naturally deformed rock. The linear clusters are not random in character as in Fry (1979). In the first case (a)–(c), one linear cluster is apparent. In the enlarged inset the empty central zone is used to determine the parameters (a, h, β) of the interpretative triangle. One well defined linear cluster is apparent with an angle of $-23°$ to the perpendicular to the S1 plane. By comparison with numerical values, a strain rate of $\gamma = 1.7$ is estimated in a dextral simple-shear hypothesis. In the second case (d)–(f), two less defined linear clusters appear (d), interpretative scheme (e) helps for perception and schematic triangle (f) gives the parameters (a, β_1, β_2).

APPLICATIONS TO ROCK DEFORMATION

The method has been applied to deformed and non deformed natural rocks. Natural samples have been chosen from various types of deformed and non-deformed peridotites. Only deformed peridotites for which olivine petrofabrics show evidence of simple shear deformation are taken into account. For peridotites we proceed in the following way (Misseri & Vigneresse 1982). Olivine porphyroclasts are only considered within an area where the grain size is homogeneous. Thin sections are cut along the plane parallel to the lineation and perpendicular to the foliation plane (XZ plane). Each crystal barycenter has been pointed out on a thin section magnifier (× 16). No intensity factor has been taken into account to include size or shape parameters of each grain, we only used binary signals. The autocorrelated diagram is directly plotted by an appropriate displacement of the coordinates of the sampled points (Fig. 2).

In the resulting autocorrelation diagram (Fig. 8a), the existence of only one type of linear clusters and a central empty zone is observed. By measuring the distance separating the linear clusters, and the half width of the central empty zone as well, the ratio a/h can be calculated. The angle between the linear cluster and the perpendicular to the foliation plane is also determined. The foliation plane is defined with respect to the shear plane determined from subboundaries in olivine grains which also give the shear sense (Nicolas & Poirer 1976). All those parameters are used to characterize the average minimum triangular mesh. An identical process may be followed for the determination of the angles β_1 and β_2 in the case of two weakly defined linear clusters (Fig. 8b). Those parameters allow a comparison with numerically simulated lattice deformation.

When applied to deformed peridotite, the autocorrelation diagram (Fig. 8a) displays a well defined linear cluster oriented $-23°$ to the perpendicular to the foliation plane ($S1$). At the centre of the diagram, an empty

zone is present, allowing the determination of the ratio $a/h = 0.28$. Comparison with the numerically simulated triangular mesh deformation through the templates (Figs. 5 and 7), the mean strain value applied to the sample is found about $\gamma = 1.7$ in the case of simple shear. No check can be made about the value of strain obtained since no quantitative strain estimating method exists for such rocks. However, qualitative field observations agree with a moderate strain value suffered by the region.

The error is estimated to be about 20% and mainly depends on the starting mesh of the sample. Precision is a function of the point distribution. It depends strongly on the accuracy of measurement of the various parameters and estimation of the distances between clusters.

DISCUSSION

The starting hypotheses which effectively limit the applicability of the method are now discussed.

All the obtained autocorrelation diagrams have shown a linear cluster organization, though Fry (1979) and Ribeiro *et al.* (1983) have not observed such a process and rather obtained random diagrams. In fact these authors assumed an isotropic process such that the local pseudo-lattice is passive during deformation: the markers are isotropically distributed and behave independently from the others; they do not materially interact, except from non overlapping, and they can reorientate. In the present approach an active lattice organized process is assumed since both spinels and olivine crystals are considered as more or less lattice organized. During deformation, if one crystal moves, the surrounding crystals have to accommodate the resulting displacement and react to such a process since they are connected within the lattice.

The hypothesis of an anticluster process (production of a central empty zone), has been examined in relation to the size of the sample. If the total number of points entering the signal is increased, the resulting autocorrelation diagram loses its well-defined cluster character. This may occur when the total number of points is greatly increased (over 100), leading to an autocorrelation diagram with over 10,000 points. The central empty zone is conserved and progressively spreads by Fry's (1979) process. This is due to large scale changes in the periodic character of the pseudo-lattice underlying the crystal distribution in the rocks. The average frequency is conserved, but slight rotations of the lattice may induce drastic changes in the phase component of the autocorrelated diagram.

The total number of points influences whether anticlusters or linear clusters are obtained. If too many points are taken into account, slight variations in the crystals lattice are perceived as departure from the original lattice and result in the widening of the frequency spectrum of the autocorrelated diagram. Conversely, if not enough points are entered into the process, the resolution of the average shape of the mesh (central empty zone) is not good enough. In fact the total number of points depends on the starting material and on the process which must be emphasized. Non-lattice organized-markers, such as ooliths or reduction spots, may be examined via the anticluster process since they behave independently during deformation. Grain repartition in rocks should be examined through its departure from lattice organized data.

We ideally deal with lattice or pseudo-lattice organized data, though few regular lattices are encountered in nature. Differences in grain sizes or small scale anisotropy are far more common. Even allowing a 20% departure for the points from their initial equilateral position did not substantially alter the results. Therefore we assume that a nearly equilateral (within 20% of variation for each side) pseudo-lattice mode is a good approximation to rocks provided no pronounced shape texture is present. The underlying existence of a pseudo-lattice organized rock has been tested through the same type of computation using non (or weakly) deformed natural rocks, namely peridotites from the Red Sea. When applying the method to these samples, linear clusters are observed yielding the conclusion that the starting material (natural rocks with equant grain size crystals) possessed a pseudo-lattice structure. This assumption may be verified through two-dimensional Fourier analysis of crystals in natural rocks. In such a case, the frequency spectrum should display a pronounced peak related to the average distance between grains, the half width of the peak depending upon the departure of the average grain size from the average distance between grains. Several authors have dealt with this problem, mainly in texture analysis (Whitten & Dacey 1975) or in statistical processes (Davis 1973).

Since the simulation deals with lattice organized data, it involves continuity in the interaction process between adjacent meshes. Transposed to geological conditions this would imply that grain positions are only geometrically dependent. No physical consideration is made upon discontinuous processes within the lattice such as grain migration, grain boundary sliding, pressure solution or diffusion creep.

Only low to moderate deformed materials have been used. The higher the strain, the poorer is the resolution of strain quantification, because of the tangent dependent function in the strain law. Application to any rock is obvious since no physical or rheological properties of the material have been introduced in the treatment. However, for application to other rocks, it would, however, be judicious to check the linear relationship between $\tan^{-1}\gamma$ and a/h against a possible dependence on rheological properties of the examined material.

CONCLUSIONS

An autocorrelation process applied to natural rocks and simulated deformed lattices results in linear clusters of points, each of them representing the barycentre of a crystal, the orientation of which depends upon the strain.

By computing the parameters related to those clusters, graphs are produced which can be used to estimate the strain pattern. The parameters given by the autocorrelation diagram are the distance separating the linear clusters and the half width of the central empty zone; the values of the different linear clusters orientations complete the parameters list. If the assumption is made that the starting material possesses a pseudo-lattice organization, which seems to be the case for rocks with equant grains, then the strain pattern obtained in the case of simple shear is estimated with a precision in the range of 20%. This estimate holds when one well-defined direction of clusters is obtained on the diagram provided deformation is not greater than a value of $\gamma = 3$. The method is less precise when two less-defined clusters are present, due to the more difficult estimation of their orientations. When the strain value is very high, then no precise estimate is possible. The method may also be used as complementary to the Fry (1979) and Ribeiro *et al.* (1983) methods in the case of cluster or anticluster distribution of markers in deformed rocks, since it may provide information on small-scale samples.

Acknowledgements—We acknowledge fruitful discussions with A. Nicolas and staff from the laboratory (ERA 547 from CNRS). P. R. Cobbold, N. Fry and A. Possolo greatly improved the manuscript which was originally submitted for the Rennes special issue of the *Journal of Structural Geology* (vol. **5**, no. 3/4, 1983) and edited by P. R. Cobbold. Parts of computation have been simultaneously run on Nantes university computer and Rennes' CAESS microcomputer.

REFERENCES

Agterberg, F. P. 1974. *Geomathematics*. Elsevier, Amsterdam.

Barbier, J. and Leymarie, P. 1972. Disposition reguliere de certaines mineralisations dans le granite de Mortagne (Vendee). *Bull. Bur. Rech. geol. Min.* **2**, 11–18.

Brun, J. P. 1980. The cluster ridge pattern of mantle gneiss domes in eastern Finland: evidence for large scale gravitational instability in the Proterozoic crust. *Earth Planet. Sci. Lett.* **47**, 441–449.

Davis, J. C. 1973. *Statistics and Data Analysis in Geology*. Wiley, New York.

Fry, N. 1979. Random points distributions and strain measurements in rocks. *Tectonophysics* **60**, 89–105.

Hanna, S. & Fry, N. 1979. A comparison of strain determination in rocks from southwest Dyfed (Pembrokeshire) and adjacent areas. *J. Struct. Geol.* **1**, 155–162.

Julesz, B. 1962. Visual pattern discrimination. *IRE Trans. Information theory* **IT-8**, 84–92.

Kulhanek, O. 1976. *Introduction to Digital Filtering in Geophysics*. Elsevier, Amsterdam.

Misseri, M. & Vigneresse, J. L. 1982. Autocorrelation des positions du spinelle dans les peridotites: liaison avec la deformation. *C. r. hebd. Séanc. Acad. Sci. Paris* **295**, 1015–1018.

Nicolas, A. and Poirier, J. P. 1976. *Crystalline Plasticity and Solid State Flow in Metamorphic Rocks*. Wiley, New York.

Ramsay, J. G. 1967. *Folding and Fracturing of Rocks*. Mc-Graw Hill, New York.

Ramsay, J. G. 1980. Shear zone geometry: a review. *J. Struct. Geol.* **2**, 83–99.

Robinson, E. A. 1967. *Statistical Communication and Detection with Special Reference to Digital Data Processing of Radar and Seismic Signals*. Griffin. 368 pp.

Ribeiro, A., Kullberg, M. C. & Possolo, A. 1983. Finite strain estimation using anticlustered distributions of points. *J. Struct. Geol.* **5**, 233–243.

Whitten, E. H. T. and Dacey, M. F. 1975. On the significance of certain Markovian features of granite textures. *J. Petrol.* **16**, 429–453.

APPENDIX

We deal with a hexagonal compact lattice. Each mesh may be viewed as a combination of six elementary triangular meshes. Thus, each point X_j of the elementary hexagon has coordinates (x_j, y_j), where

$$X_j = a \exp(i\alpha_j) = \begin{vmatrix} a\cos\alpha_j \\ a\sin\alpha_j \end{vmatrix}$$

a is the lattice parameter and $\alpha_j = j(\pi/6) + \phi$, with ϕ the angle between the stacking plane and Ox the reference axis. Distances and azimuth of each internal line may be calculated as follows:

$$d_{jk} = \|X_j - X_k\| \quad \theta_{jk} = \mathrm{Arg}\{\exp[i(\alpha_j - \alpha_k)]\}.$$

Two dimensional deformation can be simulated through a general matrix representation. In that case the general formula (Ramsay 1980) is

$$D = \begin{vmatrix} a + b\gamma & b + d\gamma \\ b(1+\Delta) & d(1+\Delta) \end{vmatrix}$$

where a, b and c represent the terms of the homogeneous deformation gradient matrix. For the case of homogeneous plane strain with no volume change, this reduces to ($a = 1$, $b = 0$, $\Delta = 0$).

$$D = \begin{vmatrix} 1 & \gamma \\ 0 & 1 \end{vmatrix}.$$

The distance between two points of the lattice is

$$d_{ik}^2 = a^2[\gamma^2(\sin\alpha_i - \sin\alpha_k)^2 + \gamma\{\sin 2\alpha_i + \sin 2\alpha_k - 2\sin(\alpha_i + \alpha_k) + 2 - 2\cos(\alpha_i - \alpha_k)\}].$$

The angle of the line between two points and the shear plane is

$$\theta_{jk} = \frac{\cos\alpha_j - \cos\alpha_k}{\sin\alpha_j - \sin\alpha_k} + \gamma.$$